IEEE Access
Multidisciplinary | Rapid Review | Open Access Journal

Received January 18, 2019, accepted February 17, 2019, date of publication February 25, 2019, date of current version March 12, 2019.

Digital Object Identifier 10.1109/ACCESS.2019.2901577

Submillimeter Wave High Order Frequency Multiplier Based on Graphene

SAMUEL VER HOEYE, (Member, IEEE), ANDREEA HADARIG, CARLOS VÁZQUEZ, MIGUEL FERNÁNDEZ, LETICIA ALONSO, (Student Member, IEEE), AND FERNANDO LAS HERAS, (Senior Member, IEEE)

Signal Theory and Communications Group, Department of Electrical Engineering, University of Oviedo, 33203 Gijón, Spain

Corresponding author: Carlos Vázquez (vazquezcarlos@uniovi.es)

This work was supported in part by the European Union Seventh Framework Programme (FP/2007-2013) under Grant 600849, in part by the Spanish Agencia Estatal de Investigación (AEI), in part by the Fondo Europeo de Desarrollo Regional (FEDER), under Grant TEC2016-80815-P (AEI/FEDER,UE), Grant TEC2015-72110-EXP (AEI), Grant AP2012-2020, and Grant FPU14/00016, and in part by the Gobierno del Principado de Asturias (PCTI/FEDER-FSE), under Grant IDI/2016/000372, Grant IDI/2017/000083, and Grant BP13034.

ABSTRACT In this paper, a single stage millimeter/submillimeter wave frequency multiplier is presented. The desired frequency multiplication performance is obtained through the nonlinear excitation of high-order harmonic components in a graphene film, when it is illuminated with a low-frequency input signal. The graphene film is integrated into a microstrip structure on a polyimide substrate, which is subsequently embedded in a micromachined waveguide block. The design has been optimized to receive an input signal in the Ka frequency band, between 26.5 and 40 GHz, and to produce an output signal in the WR-3 frequency band, between 220 and 330 GHz. A complete prototype of the frequency multiplier module, including standard waveguide flanges for its interconnection, has been manufactured and experimentally characterized. The results in terms of output power in the WR-3 frequency band, for harmonic orders between 6 and 11, as well as for input power levels between 7 and 21 dBm, are presented.

INDEX TERMS Frequency multiplier, graphene, millimeter wave circuits, submillimeter wave circuits, nonlinear circuits.

I. INTRODUCTION

In recent years, the benefits of exploiting the properties of electromagnetic radiation and its propagation characteristics in the submillimeter wave and lower THz frequency bands have been extensively described [1], [2]. A wide variety of potential applications in fields as diverse as security, medical diagnostics or nondestructive testing, among many others, has been proposed [3]–[7]. Despite the great number of potential applications, the cost-effective signal generation at these frequency bands still represents a technological bottleneck, which strongly conditions the development of practical implementations. The most common approach to signal generation in the submillimeter wave and lower THz frequency bands is the frequency multiplication through harmonic excitation in nonlinear solid state devices, such as Schottky diodes. While relatively high efficiencies have been obtained with these topologies for low multiplications orders (i.e. 2 and 3) [8]–[11], as summarized in Table 1, in terms of maximum output power P_o and conversion gain G_c. However, these values tend to drop rapidly when increasing the multiplication order N. Therefore, diode based frequency multipliers intended to reach the submillimeter and THz band are usually implemented by interconnecting several low order multipliers and power amplifiers in cascaded multistage topologies [11], [12], leading to a higher cost and lower power efficiency.

As opposed to solid-state devices, graphene sheets have been theoretically predicted to generate unlimited and slowly decaying harmonic components when excited with an external electric field [13], [14]. Moreover, due to the linear energy dispersion of its electrons and holes, graphene is intrinsically a strongly nonlinear material, capable of generating high order harmonic content from incident field levels several orders of magnitude smaller than those required in many other nonlinear materials [15]–[17]. Due to these features, graphene is an excellent alternative for high order frequency multiplication.

Implementations of frequency multipliers using novel graphene based field effect transistors have been reported

The associate editor coordinating the review of this manuscript and approving it for publication was Vittorio Camarchia.

TABLE 1. Solid state frequency multipliers found in the literature.

Ref.	f_o (GHz)	N	Max. P_o (dBm)	Max. G_c (dB)
[8]	170 – 190	2	17.8	-4.3 (180 GHz)
[10]	67 – 110	3	3	-16 (75 GHz)
	50 – 110	2	6.8	-12 (50 GHz)
[11]	170 – 190	2	14.8	-4.6 (180 GHz)
	350 – 370	2	9.5	-7 (360 GHz)

in [18]–[22]. Nevertheless, these devices generally focus on the second or third multiplication order, not fully exploiting the capability of graphene to efficiently generate higher order harmonic content. On the other hand, the capability of graphene sheets, integrated in a coplanar waveguide [23] or microstrip structure, to directly generate high order harmonic components has been experimentally demonstrated in [24]–[31], at millimeter/submillimeter wave frequencies.

In [31], a preliminary millimeter/submillimeter wave frequency multiplier design, integrated with a horn antenna, was illustrated for the frequency conversion between the Ka band (26.5-40 GHz) and the WR-3 frequency band (220-330 GHz). A prototype was fabricated in plastic through a stereolithography process and subsequently metallized in a gold sputtering process.

In this work, the preliminary design presented in [31] has been optimized, leading to a single-stage high-order millimeter/submillimeter wave frequency multiplier, which has been manufactured as a complete module including standard input and output waveguide flanges, through a micromachining process. The design integrates a multilayer graphene film in a microstrip transmission line terminated by two back-to-back microstrip to rectangular waveguide transitions. The multiplier performance has been comprehensively characterized for different harmonic orders and versus the input power level.

The paper is organized as follows. In Section II, the topology of the graphene based frequency multiplier is introduced. In Section III, the design and optimization process is described. Section IV is dedicated to the experimental characterization of the frequency conversion performance. Finally, in Section V, some conclusions are presented.

II. MULTIPLIER TOPOLOGY

The topology of the single stage high order frequency multiplier is illustrated in Fig. 1a. The circuit is composed of a waveguide block and a microstrip structure integrating a multilayer graphene film. The input signal, in the Ka frequency band, is provided through a WR-28 waveguide to microstrip transition. The output signal, in the 220-330 GHz frequency band, which is a harmonic component of the input signal generated in the graphene film, is delivered to the standard WR-3 output waveguide, through a microstrip to rectangular waveguide transition. In order to achieve a good impedance matching at the input port over the whole Ka

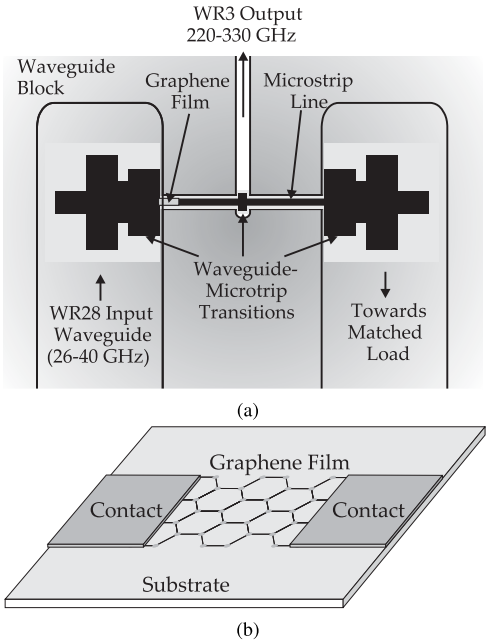

FIGURE 1. Graphene based frequency multiplier. (a) Topology. (b) Microstrip line with graphene film.

frequency band, a path is provided for the input signal through the microstrip structure towards a second WR-28 waveguide section terminated in a waveguide matched load.

The graphene film integrated in the microstrip structure is prepared by mechanical exfoliation of Highly Oriented Pyrolytic Graphite (HOPG) [24]–[26], [28]. Metallic contacts, as depicted in Fig. 1b, are deposited on top of the graphene film by gold sputtering, leaving a 150 µm gap uncovered. The dielectric substrate employed for the microstrip structure is 50 µm thick polyimide (Kapton) with dielectric constant $\varepsilon_r = 3.5$ and $\tan\delta = 0.008$.

The microstrip structure includes three waveguide to microstrip transitions connected through a high impedance transmission line, enclosed in a metallic channel with rectangular cross section (Fig. 1a). The dimensions of that cross section must be selected to suppress the propagation of waveguide modes at the operating frequency. Taking advantage of the decrease in operating frequency with regard to [28], a channel cross section of 0.41 mm × 0.12 mm was chosen in this work, enabling the use of a 50 µm substrate for the microstrip structure, instead of the 25 µm substrate required in [28]. The complete redesign of the microstrip structure integrating the graphene film and the microstrip to waveguide transitions for this substrate thickness resulted in a significant simplification of the associated fabrication, handling and assembly processes. Moreover, the increased thickness confers improved mechanical and thermal stability to the assembled prototype.

III. DESIGN AND OPTIMIZATION OF THE FREQUENCY MULTIPLIER

The graphene based frequency multiplier has been designed and optimized using the three-dimensional electromagnetic

simulator Ansoft HFSS. An optimization process based on the following two steps has been used.

A. SUBMILLIMETER WAVE BAND OPTIMIZATION

The design process is started with the optimization of the submillimeter wave section composed by the microstrip to WR-3 rectangular waveguide transition, the feeding microstrip line, and the output WR-3 rectangular waveguide (Fig. 2a).

The shape of the microstrip structure, its position, and the dimensions of a reduced height section of the WR-3 waveguide in the proximity of the microstrip transition, are optimized to obtain maximum power transfer from the input Port 1 towards the output Port 3. The microstrip line is embedded in a metallic channel whose dimensions have been chosen to be 0.41 mm $\times$ 0.12 mm, in order to prevent the propagation of undesired waveguide modes. The width of the microstrip line is 130 μm, corresponding to a 50 Ω characteristic impedance.

The simulated scattering parameters of the optimized transition are shown in Fig. 2b. The transmission loss between the output Port 3 and the input Port 1 is approximately 5 dB, partly due to the power transported towards Port 2 and partly due to the dielectric loss in the Kapton substrate and the ohmic losses in the microstrip structure. The reflection coefficient at the input port is below −10 dB in the 220-320 GHz frequency band, assuring a good impedance matching.

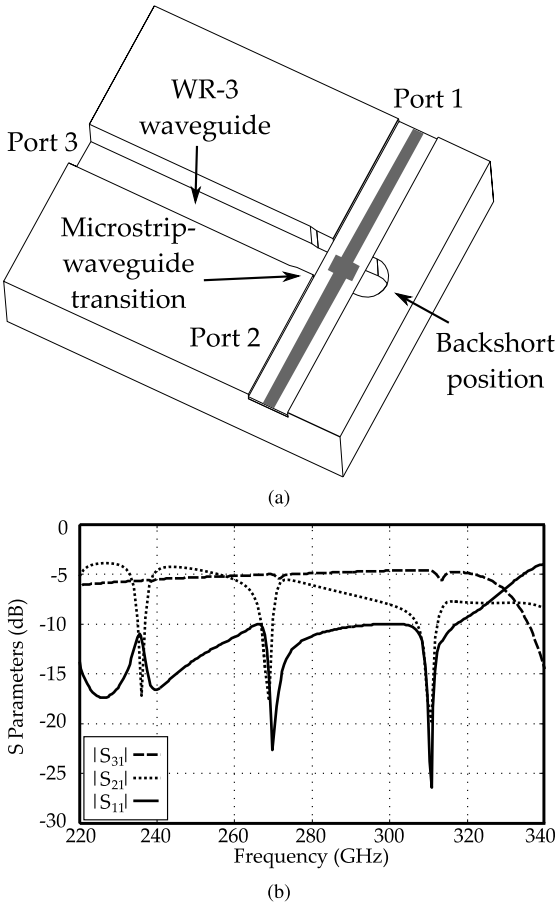

FIGURE 2. Microstrip line to WR3 rectangular waveguide transition: (a) Topology. (b) Scattering parameters.

B. MILLIMETER WAVE BAND OPTIMIZATION

In a second design stage, the complete frequency multiplier design is optimized in the Ka frequency band. For this purpose, the microstrip to WR-3 rectangular waveguide transition, optimized in the previous stage, is inserted and left unmodified in the complete frequency multiplier design. As presented in Fig. 3a, the topology used to analyze the frequency multiplier in the Ka band consists of two WR-28 waveguides and two microstrip segments connected to the microstrip to WR-3 waveguide transition. The complete microstrip structure, which will integrate the graphene film, is terminated with two WR-28 waveguide to microstrip transitions. Those transitions consist of a microstrip structure including stubs and several successive microstrip sections with low and high impedance. Additionally, multiple reduced and increased height sections are introduced in the WR-28 waveguides to achieve broadband performance. Due to limitations in the fabrication process, the design has been modelled with rounded corners with a minimum radius of 0.4 mm.

The simulated scattering parameters of the optimized transition are shown in Fig. 3b. Good impedance matching at the input, Port 1, with a reflection coefficient lower than −10 dB in the 28 - 40 GHz frequency band was obtained. The power loss between the two WR-28 waveguide ports 1 and 2 is below 4 dB.

IV. EXPERIMENTAL CHARACTERIZATION

A. PROTOTYPE IMPLEMENTATION

For the evaluation of the behavior of the graphene based frequency multiplier, a prototype of the complete design has been manufactured and experimentally characterized.

The waveguide structure, including the input WR-28 and output WR-3 waveguide sections and the channel between them, is composed of several 1 mm thick brass sheets, which were micromachined separately. Standard WR-28 (type UG-387/UM) and WR-3 (type UG-599/U) flanges were subsequently soldered to the assembled waveguide structure.

B. GRAPHENE FILM INTEGRATION

The graphene film is integrated in a gap on the microstrip segment between the WR-28 and WR-3 waveguide transitions, where a maximum tangential electric field level is observed.

A few-layer graphene film is mechanically exfoliated from a HOPG block with conductivity values, as declared by the manufacturer, of 2.1 MS/m and 500 S/m in the directions parallel and perpendicular to the layer surface, respectively. The exfoliated layer is transferred onto the polyimide substrate using a polymethylmethacrylate (PMMA) film.

The shape of the graphene film is subsequently patterned using a laser ablation process. The width of the graphene film is chosen to be the same as the width of the microstrip line

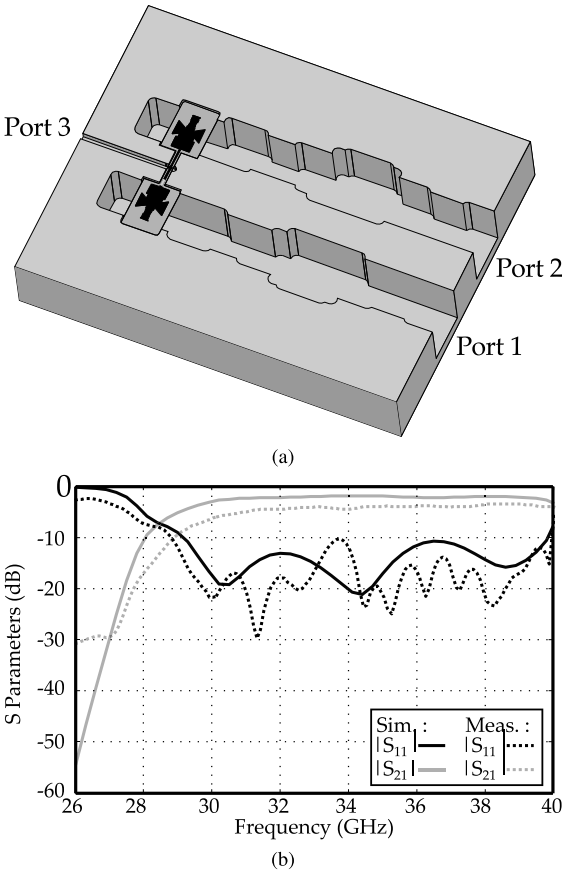

FIGURE 3. Frequency multiplier simulated in the Ka frequency band: (a) Topology. (b) Scattering parameters.

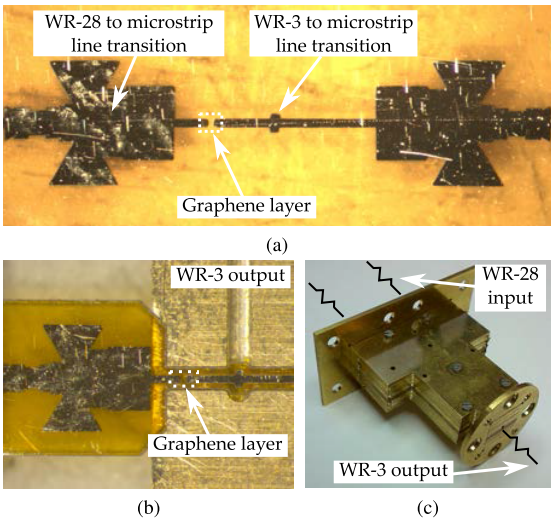

FIGURE 4. Prototype of the graphene based frequency multiplier: (a) Microstrip line structure. (b) Microstrip structure placed into the waveguide block. (c) Assembled prototype.

inside the channel, in order to facilitate the transport of the submillimeter wave signal towards the WR-3 output port.

A 1 μm thick gold layer is sputtered on the polyimide substrate, simultaneously creating the metallic contacts to the graphene film and the microstrip structure, which is finally etched in the desired shape through a lift off process (Fig. 4a).

The same laser ablation process employed to pattern the graphene film is used to cut out the supporting polyimide substrate. The complete microstrip structure is subsequently mounted onto the waveguide block (Fig. 4b), using pick and place equipment. The completed frequency multiplier prototype is shown in Fig. 4c.

C. MEASUREMENT SETUP

The frequency multiplication behavior of the prototype has been characterized using the experimental setup presented in Fig. 5. The input signal, generated by a Keysight PNA-X vector network analyzer and amplified by a 30 dB gain power amplifier, is delivered to one of the WR-28 waveguide sections of the frequency multiplier, through a Keysight R281A coaxial to waveguide adapter. A 50 Ω load is connected to the other WR-28 waveguide port by means of a Keysight R281B coaxial to waveguide adapter.

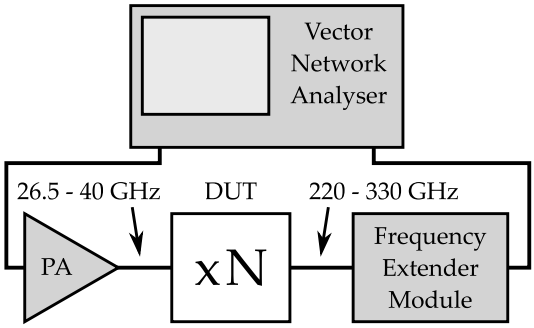

FIGURE 5. Schematic diagram of the measurement setup.

The output signal of the frequency multiplier corresponding to different harmonic components with order N, has been measured with a PNA-X vector network analyzer, together with a Virginia Diodes (VDI) frequency extender (receiver) module, operating in the 220-330 GHz frequency band. The power measurement of the receiving frequency extender module has been calibrated in two steps. First, the power delivered by a VDI transmitting frequency extender module has been measured in the 220-330 GHz band, using an Erikson PM4 calorimeter-based power meter. Then, the power delivered by the same transmitting extender module has been measured by the VDI receiving extender module. By comparing both measurements, the calibration data required for the VDI receiving frequency extender module was obtained.

The input frequency band is limited by the performance of the WR-28 waveguide to microstrip transition to the range between 28 and 40 GHz. On the other hand, the output frequency band is limited by the measurement equipment to the interval from 220 to 330 GHz. Therefore, the multiplier input and output frequency bands for different harmonic orders between 6 and 11, are summarized in Table 1.

Using the experimental setup presented in Fig. 5, a calibrated measurement of the output power generated in the WR-3 band will be obtained, as a function of the available power at the input port, which is calculated from the calibrated output power of the vector network analyzer and the

calibrated gain of the power amplifier. The power effectively delivered to the frequency multiplier will only equal the available power when the frequency multiplier is operated within its input frequency band. Nevertheless, in the following sections, the available power thus calculated will be referred to as input power, for simplicity.

D. ODD ORDER HARMONIC COMPONENTS

The behavior of the graphene based frequency multiplier for different odd order harmonic components has been characterized by measuring the output signal in the 220-330 GHz frequency band, while varying the frequency and power of the input signal.

For each considered multiplication order, the power of the output signal has been evaluated versus the power of the input signal, which was varied from $P_{\text{in}} = 7$ to 21 dBm, in 2 dB steps. The measured data obtained for odd order harmonic components is represented in Fig. 6. The operation bands, as have been defined in Table 2, are indicated as shaded regions in the figures.

TABLE 2. Operation bands for the different harmonic components.

Order N	Input Frequency Range f_{IN} (GHz)	Output Frequency Range $N \times f_{IN}$ (GHz)
6	36.6 – 40	220 – 240
7	31.4 – 40	220 – 280
8	28 – 40	224 – 320
9	28 – 36.6	252 – 330
10	28 – 33	280 – 330
11	28 – 30	308 – 330

As shown in Fig. 6, the maximum power level achieved is around −32 dBm in the case of the 7$^{\text{th}}$ harmonic component, −42 dBm in the case of the 9$^{\text{th}}$ harmonic component and −59 dBm in the case of the 11$^{\text{th}}$ harmonic component. As can be verified, the performance for the 7$^{\text{th}}$ harmonic component remains stable beyond the upper limit of the shaded area, which corresponds to input frequencies greater than 40 GHz. This behavior continues up to the cutoff frequency of the input amplifier gain characteristic, at about 45 GHz, associated with an output frequency $45 \times N = 315$ GHz.

The power levels generated in the millimeter/submillimeter wave frequency band have been significantly improved with regard to [31], exhibiting a predominantly flat frequency response throughout the band corresponding to each harmonic order. The remaining small frequency fluctuations in the output power are caused by mild variations in the frequency response of the waveguide to microstrip transitions in the input and output frequency bands.

E. EVEN ORDER HARMONIC COMPONENTS

The theoretical analysis of a graphene film illuminated by an electromagnetic wave, under the particular case of normal incidence, predicts that only odd order harmonic components will be generated, due to the central symmetry of the graphene structure [15]. However, for oblique incidence or, in other words, when the incident electric field is not parallel to the graphene film, the symmetry does not preclude generation of even order components.

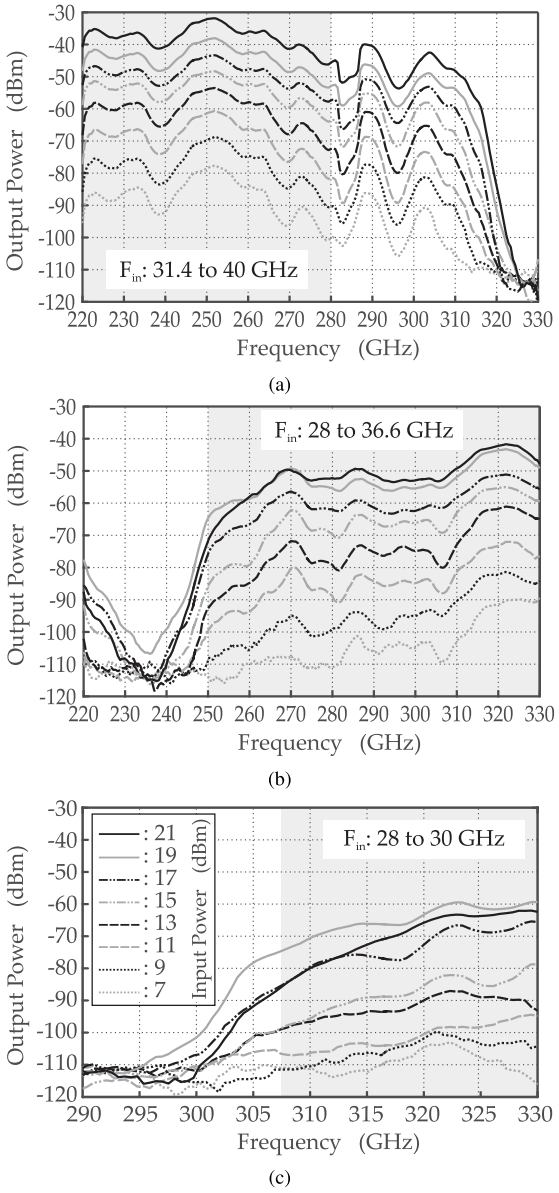

FIGURE 6. Output power for odd harmonic components. (a) Multiplication by 7. (b) Multiplication by 9. (c) Multiplication by 11. Input power considered from 7 dBm to 21 dBm varied in 2 dB steps.

The 6$^{\text{th}}$, 8$^{\text{th}}$ and 10$^{\text{th}}$ harmonic components generated in the frequency multiplier have been evaluated. The output power, in the 220-330 GHz frequency band, has been measured while varying the power of the input signal between 7 and 21 dBm, in 2 dB steps, as shown in Fig. 7.

The maximum power level achieved is around -66 dBm in the case of the 6$^{\text{th}}$ harmonic component, −68 dBm in the case of the 8$^{\text{th}}$ harmonic and −71 dBm in the case of the 10$^{\text{th}}$ harmonic component.

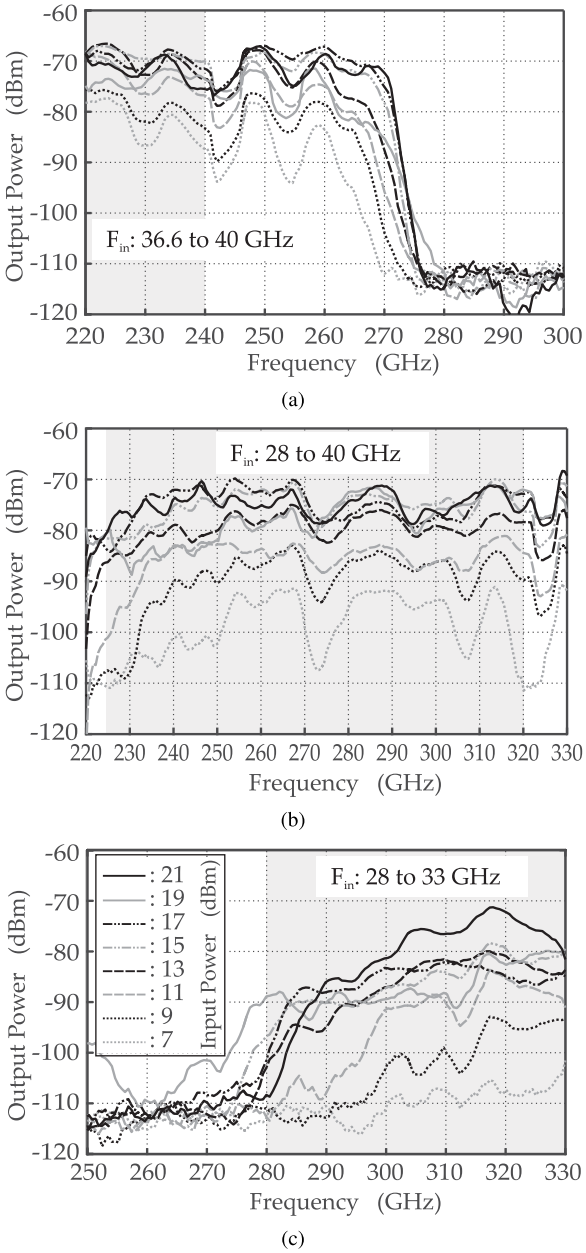

FIGURE 7. Output power for even harmonic components. (a) Multiplication by 6. (b) Multiplication by 8. (c) Multiplication by 10. Input power considered from 7 dBm to 21 dBm varied in 2 dB steps.

The output power generated at even order harmonic components of the input signal is significantly lower than that obtained at odd order harmonic components, in agreement with the theoretical predictions presented in [15]. Taking advantage of the special nonlinear properties of graphene, a wideband and relatively flat frequency response has been achieved, for both odd and even order harmonic components. Since the generation of harmonic components in graphene layers, as predicted in [15], extends from microwave up to optical frequencies, the frequency multiplier topology can be easily re-optimized for its operation in lower or higher frequency bands [28], [30].

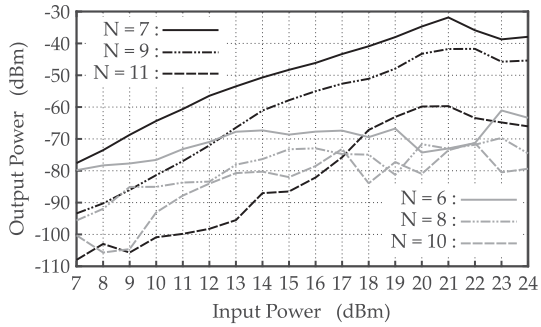

FIGURE 8. Output versus input power for different harmonic orders.

F. OUTPUT POWER SATURATION

The output power is evaluated in Fig. 8 versus the input power, for different harmonic orders N, between 6 and 11. For each harmonic component, the measurement has been performed at a single output frequency, as follows: $N = 6$: 225 GHz, $N = 7$: 252 GHz, $N = 8$: 289 GHz, $N = 9$: 322 GHz, $N = 10$: 318 GHz and $N = 11$: 322 GHz.

For odd harmonic components, an almost linear variation of the output power with respect to the input power can be observed up to an input power of 21 dBm (Fig. 8). Above this level, a saturation effect of the output power can be observed. For even harmonic components, the linear increase of the output power is only observed for lower values of the input power, and the saturation effects appear for input power levels above approximately 13 dBm.

For input power levels above 21 dBm, the heat generated in the narrow sections of the structured graphene layer causes deformations in the polyimide substrate and, in turn, mechanical stress in the graphene film, leading to an unstable behavior of the output power. Increasing the input power beyond that point led to unrecoverable damage of the graphene layer.

G. COMPARISON OF FREQUENCY MULTIPLIER PERFORMANCE

The performance of the proposed frequency multiplier is compared to other graphene based implementations that have been presented in the literature in Table 3, in terms of output frequency range, f_o, harmonic order N, maximum output power P_o and maximum conversion gain G_c.

In [19], [20], and [22], different frequency doublers have been proposed using graphene-based FET transistors for their operation in the microwave band under 8 GHz. With these designs, maximum output power values between -25 dBm and -22.5 dBm and maximum conversion gain values between -35 dB and -28 dB have been achieved.

In [24], a frequency tripler based on a microstrip gap with a multi-layer graphene sheet is presented for operation up to 15 GHz. With this configuration, a higher maximum output power, $P_o = -9$ dBm, and conversion gain, $G_c = -26$ dB, were obtained.

In [23], the frequency multiplication effect in a metallic coplanar waveguide (CPW) deposited directly on a DC biased graphene monolayer is demonstrated for harmonic orders

TABLE 3. Comparison with other graphene-based frequency multiplier designs presented in the literature.

Ref.	f_o (GHz) (GHz)	N	Max. P_o (dBm)	Max. G_c (dB)
[19]	$0.1-1.5$	2	-25	-31
[23]	$2-30$	$2-7$	-37 ($N=2$, 2 GHz)	-37 ($N=2$, 2 GHz)
[24]	$7.5-15$	3	-9	-26
[20]	$0-3$	2	-25	-35
[22]	$2-8$	2	-22.5	-28
[27]	$230-255$	7	-50	-80
[28]	$330-500$	$9-17$	-36 ($N=9$, 355 GHz)	-60 ($N=9$, 355 GHz)
This Work	$220-330$	$6-11$	-34 ($N=7$, 250 GHz)	-55 ($N=7$, 250 GHz)

from 2 to 7 and signal generation up to 30 GHz. With this topology, for harmonic order 2, a maximum output power of -37 dBm and conversion gain of -37 dB has been obtained at a 2 GHz output frequency. However, for order 7, those values reduce to -57 dBm and -58.4 dB, respectively, for an output frequency of 7 GHz.

For operation in the millimeter and submillimeter wave bands, graphene based frequency multipliers have been proposed using topologies similar to that presented in this work. In [27] a frequency multiplier by 7 is presented with an operation band between 230 GHz and 255 GHz. With this design, the values obtained for the output power (-50 dBm) and conversion gain (-80 dB) are considerably lower than the ones obtained at microwave frequencies. In [28] a design has been presented in the band between 330 GHz and 500 GHz, using harmonic orders from 9 to 17. The maximum output power and conversion gain achieved at 355 GHz was -36 dBm and -60 dB respectively.

In this work, with the proposed frequency multiplier, using harmonic orders between 7 and 11, the full WR-3 band has been covered. Considering the high order of the harmonics used for the frequency multiplication, a high output power and conversion gain has been obtained in a single multiplication stage. Note that in [23], the input and output signals are applied and measured directly on-wafer, minimizing the path between the device and the measurement probes. Conversely, the results presented in this work correspond to a complete module with standard input and output waveguide flanges, leading to longer signal paths and additional power losses.

V. CONCLUSION

A graphene based millimeter/submillimeter wave frequency multiplier capable of generating signals in the 220-330 GHz frequency band has been presented. The device exploits the nonlinear electromagnetic response of graphene to generate high order harmonic components of the input signal in a single stage, reducing its size and cost. A prototype has been implemented and experimentally characterized. The variation of the output power versus the input power has been analyzed, considering different multiplication orders. It has been observed that the bandwidth of the multiplier is mainly limited by the circuitry surrounding the graphene layer, allowing future designs at high or lower frequency bands. The measured output power at odd order harmonic components was considerably higher than at even order harmonics, in accordance with previously reported theoretical analyses.

REFERENCES

[1] J. E. Pedersen and S. R. Keiding, "THz time-domain spectroscopy of nonpolar liquids," *IEEE J. Quantum Electron.*, vol. 28, no. 10, pp. 2518–2522, Oct. 1992.

[2] K. Fukunaga, "THz technology applied to cultural heritage," in *Proc. Int. Conf. Infr., Millim., Thz Waves*, Wollongong, NSW, Australia, Sep. 2012, pp. 1–4.

[3] B. Zhu, Y. Chen, K. Deng, W. Hu, and Z. S. Yao, "Terahertz science and technology and applications," in *Proc. PIERS*, Mar. 2009, pp. 1166–1170.

[4] J. H. Son, *Terahertz Biomedical Science and Technology*. Boca Raton, FL, USA: CRC Press, 2014.

[5] I. Hosako and K. Fukunaga, "Non destructive observation of defects in dielectric materials and prospects for diagnostics of infrastructure and cultural heritage," in *Proc. 30th URSI Gen. Assem. Sci. Symp.*, Istanbul, Turkey, Aug. 2011, pp. 1–4.

[6] Y. C. Shen and P. F. Taday, "Development and application of terahertz pulsed imaging for nondestructive inspection of pharmaceutical tablet," *IEEE J. Sel. Topics Quantum Electron.*, vol. 14, no. 2, pp. 407–415, Mar. 2008.

[7] Y. Álvarez *et al.*, "Submillimeter-wave frequency scanning system for imaging applications," *IEEE Trans. Antennas Propag.*, vol. 61, no. 11, pp. 5689–5696, Nov. 2013.

[8] C. Viegas *et al.*, "A 180-GHz Schottky diode frequency doubler with counter-rotated *E*-fields to provide in-phase power-combining," *IEEE Microw. Wireless Compon. Lett.*, vol. 28, no. 6, pp. 518–520, Jun. 2018.

[9] J. V. Siles *et al.*, "A single-waveguide in-phase power-combined frequency doubler at 190 GHz," *IEEE Microw. Wireless Compon. Lett.*, vol. 21, no. 6, pp. 332–334, Jun. 2011.

[10] M. Hrobak, M. Sterns, M. Schramm, W. Stein, and L.-P. Schmidt, "Design and fabrication of broadband hybrid GaAs Schottky diode frequency multipliers," *IEEE Trans. Microw. Theory Techn.*, vol. 61, no. 12, pp. 4442–4460, Dec. 2013.

[11] H. Liu *et al.*, "A high-power Schottky diode frequency multiplier chain at 360 GHz for gyro-TWA applications," in *Proc. 10th UK-Eur.-China Workshop Millim. Waves THz Technol. (UCMMT)*, Liverpool, U.K., Sep. 2017, pp. 1–2.

[12] T. W. Crowe, S. A. Retzloff, C. Pouzou, and J. L. Hesler, "Multiplier based sources for frequencies above 2 THz," in *Proc. 36th Int. Conf. Infr., Millim. THz. Waves (IRMMW-THz)*, Houston, TX, USA, Oct. 2011, p. 1.

[13] A. K. Geim and K. S. Novoselov, "The rise of graphene," *Nature Mater.*, vol. 6, no. 3, pp. 183–191, 2007.

[14] N. Campos *et al.*, "A comparison of the performance of micro- and nanosecond laser in micropatterning of graphene films," in *Proc. Graphene Week*, Bilbao, Spain, 2013, p. 1.

[15] S. A. Mikhailov, "Non-linear electromagnetic response of graphene," *Europhys. Lett.*, vol. 79, p. 27002, Jun. 2007.

[16] S. A. Mikhailov and K. Ziegler, "Nonlinear electromagnetic response of graphene: Frequency multiplication and the self-consistent-field effects," *J. Phys., Condens. Matter*, vol. 20, Aug. 2008, Art. no. 384204.

[17] S. A. Mikhailov, "Quantum theory of the third-order nonlinear electrodynamic effects of graphene," *Phys. Rev. B, Condens. Matter*, vol. 93, no. 8, 2016, Art. no. 085403.

[18] E. Camargo, *Microwave and Millimeter-wave FET Frequency Mulipliers and Harmonic Oscillators*. London, U.K.: Artech House, 1998.

[19] H. Wang, A. Hsu, K. K. Kim, J. Kong, and T. Palacios, "Gigahertz ambipolar frequency multiplier based on CVD graphene," in *IEDM Tech. Dig.*, Dec. 2010, pp. 23.6.1–23.6.4.

[20] M. E. Ramón *et al.*, "Three-gigahertz graphene frequency doubler on quartz operating beyond the transit frequency," *IEEE Trans. Nanotechnol.*, vol. 11, no. 5, pp. 877–883, Sep. 2012.
[21] H. Lv *et al.*, "Inverted process for graphene integrated circuits fabrication," *Nanoscale*, vol. 6, no. 11, pp. 5826–5830, 2014.
[22] H. Lv *et al.*, "Monolithic graphene frequency multiplier working at 10 GHz range," in *Proc. Int. Symp. VLSI Technol., Syst. Appl.*, Apr. 2014, pp. 1–2.
[23] M. Dragoman *et al.*, "Millimeter-wave generation via frequency multiplication in graphene," *Appl. Phys. Lett.*, vol. 97, no. 9, 2010, Art. no. 093101.
[24] R. Camblor *et al.*, "Microwave frequency tripler based on a microstrip gap with graphene," *J. Electromagn. Waves Appl.*, vol. 25, nos. 14–15, pp. 1921–1929, 2011.
[25] G. Hotopan *et al.*, "Millimeter wave microstrip mixer based on graphene," *Prog. Electromagn. Res.*, vol. 118, pp. 57–69, Aug. 2011.
[26] G. Hotopan *et al.*, "Millimeter wave subharmonic mixer implementation using graphene film coating," *Prog. Electromagn. Res.*, vol. 140, pp. 781–794, Aug. 2013.
[27] A. Hadarig *et al.*, "7^{th} order sub-millimeter wave frequency multiplier based on graphene implemented using a microstrip between two rectangular waveguides," in *Proc. Int. Conf. Electromagn. Adv. Appl.*, 2014, pp. 757–760.
[28] A. Hadarig *et al.*, "Experimental analysis of the high-order harmonic components generation in few-layer graphene," *Appl. Phys. A, Solids Surf.*, vol. 118, no. 1, pp. 83–89, 2015.
[29] C. V. Antuña *et al.*, "High-order subharmonic millimeter-wave mixer based on few-layer graphene," *IEEE Trans. Microw. Theory Techn.*, vol. 63, no. 4, pp. 1361–1369, Apr. 2015.
[30] S. Ver Hoeye *et al.*, "Graphene based THz electromagnetic imaging system for the analysis of artworks," *IEEE Access*, vol. 6, pp. 66459–66467, 2018. doi: 10.1109/ACCESS.2018.2879161.
[31] C. V. Antuña *et al.*, "Millimetre wave transmitter based on a few-layer graphene frequency multiplier," in *Proc. Eur. Microw. Conf. (EuMC)*, Paris, France, Sep. 2015, pp. 510–513.

SAMUEL VER HOEYE (M'05) received the M.Sc. degree in electronics engineering from the University of Gent, Gent, Belgium, in 1999, and the Ph.D. degree from the University of Cantabria, Santander, Spain, in 2002.

He is currently an Associate Professor with the Department of Electrical and Electronic Engineering, University of Oviedo, Gijón, Spain. His current research interests include the design and analysis of microwave, millimeter wave, and THz circuits and systems. Among these are the multi-functional oscillator-based circuits and antennas, frequency scanning antennas, graphene-based frequency multipliers and mixers, imaging systems, and textile integrated high frequency components.

ANDREEA HADARIG received the B.Sc. degree in telecommunication engineering from the Technical University of Cluj-Napoca, Romania, in 2012, and the M.Sc. degree in information technology and mobile communications and the Ph.D. degree from the University of Oviedo, Spain, in 2013 and 2017, respectively.

Since 2012, she has been a Research Assistant with the Signal Theory and Communications Group, University of Oviedo. Her current research interests include the design, optimization, and analysis of passive devices using waveguides and microstrip technology operating in the millimeter/submillimeter wave and THz frequency bands.

CARLOS VÁZQUEZ received the M.Sc. degree in telecommunication engineering, the M.Sc. degree in information technology and mobile communications, and the Ph.D. degree from the University of Oviedo, Gijón, Spain, in 2007, 2008, and 2013, respectively.

From 2007 to 2012, he was a Graduate Research Assistant with the University of Oviedo, where he has been a Research Fellow with the Signal Theory and Communications Group since 2012. His current research interests include nonlinear analysis and optimization techniques for the design of multifunctional oscillator-based circuits, active antennas and passive components, such as frequency multipliers and harmonic mixers, at microwave, millimeter/submillimeter-wave, and terahertz frequencies.

MIGUEL FERNÁNDEZ received the M.Sc. degree in telecommunication engineering, the M.Sc. degree in information technology and mobile communications, and the Ph.D. degree from the University of Oviedo, Gijón, Spain, in 2006, 2010, and 2010, respectively.

From 2006 to 2008, he was a Research Fellow, with the Signal Theory and Communications Group, University of Oviedo, where he has been an Associate Professor since 2008. His current research interests include nonlinear analysis and optimization techniques for the design of oscillator-based circuits, active antennas and frequency multipliers and mixers at the microwave, millimeter/submillimeter wave, and terahertz frequency bands.

LETICIA ALONSO received the M.Sc. degree in telecommunication engineering from the University of Oviedo, Gijón, Spain, in 2014, the M.Sc. degree in systems and control engineering from the National University of Distance Learning (UNED) and the Universidad Complutense de Madrid, Spain, in 2018, and the Ph.D. degree from the University of Oviedo, in 2018.

Since 2014, she has been a Researcher with the Signal Theory and Communications Group, University of Oviedo. She was a Visiting Scholar with the George Green Institute for Electromagnetics Research, University of Nottingham, U.K., in 2017. Her current research interests include the design, simulation, and manufacturing techniques to develop microwave and millimeter wave passive circuits and antennas fully integrated in textile technology.

FERNANDO LAS HERAS received the M.S. and Ph.D. degrees in telecommunication engineering from the Tech University of Madrid (UPM), 1987 and 1990, respectively. From 1988 to 1990 and from 1991 to 2002, he was a National Graduate Research Fellow and an Associate Professor with the Department of Signal, Systems and Radiocom of UPM and also has been a Full Professor with the University of Oviedo, since 2003. Since 2001, he has been the Head of the Research Group Signal Theory and Comm (TSC-UNIOVI), Department of Electrical Engineering, University of Oviedo. From 2004 to 2008, he was the Vice Dean for telecommunication engineering with the Tech School of Engineering, Gijón. He was a Visiting Researcher with Syracuse University, New York, also a Visiting Lecturer with the National University of Engineering, Lima, and ESIGELEC, France. From 2005 to 2015, he held the Telefónica Chair (on RF Technologies, ICTs applied to environment and climate change, and ICTs and Smartcities). He has authored more than 450 technical journal and conference papers in electromagnetic radiation, propagation and scattering theory and applications, and inverse problems. From 2012 to 2015, he was a member of the Board of Directors of the IEEE Spain Section, from 2016 to 2018, he was a member of the Board IEEE Microwaves and Antennas Propagation Chapter (AP03/MTT17), and a member of the Science, Technology and Innovation Council of Asturias, Spain, in 2010.